

CoSimGNN: Towards Large-scale Graph Similarity Computation

Haoyan Xu, Runjian Chen*

Ziheng Duan, Jie Feng

{haoyanxu,rjchen}@zju.edu.cn

{duanziheng,zjucse_fj}@zju.edu.cn

College of Control Science and Engineering,
Zhejiang University

Yunsheng Bai*

Yizhou Sun, Wei Wang

{yba,yzsun,weiwang}@cs.ucla.edu

Department of Computer Science,
University of California, Los Angeles

ABSTRACT

The ability to compute similarity scores between graphs based on metrics such as Graph Edit Distance (GED) is important in many real-world applications, such as 3D action recognition and biological molecular identification. Computing exact GED values is typically an NP-hard problem and traditional algorithms usually achieve an unsatisfactory trade-off between accuracy and efficiency. Recently, Graph Neural Networks (GNNs) provide a data-driven solution for this task, which is more efficient while maintaining prediction accuracy in small graph (around 10 nodes per graph) similarity computation. Existing GNN-based methods, which either respectively embed two graphs (lack of low-level cross-graph interactions) or deploy cross-graph interactions for whole graph pairs (redundant and time-consuming), are still not able to achieve competitive results when the number of nodes in graphs increases. In this paper, we focus on similarity computation for large-scale graphs and propose the "embedding-coarsening-matching" framework, which first embeds and coarsens large graphs to coarsened graphs with denser local topology and then deploys fine-grained interactions on the coarsened graphs for the final similarity scores. In the first two stages of our model, there is no interaction across graphs so the time complexity of this part is linear with respect to the number of nodes and edges. Meanwhile the fine-grained cross-graph interactions in matching part guarantees the performance, which is even better than directly applying cross-graph interactions on whole graph pairs. Furthermore, we propose a novel graph pooling method ADAPTIVE POOLING and create several synthetic datasets with different sizes which provide new benchmarks for graph similarity computation. Detailed experiments on both synthetic and real-world datasets have been conducted and our proposed framework achieves the best performance while the inference time is at most 1/3 of that of previous state-of-the-art.

KEYWORDS

graph similarity computation, large-scale, graph coarsening, graph deep learning

1 INTRODUCTION

With flexible representative abilities, graphs have a broad range of applications in various fields, such as social network study, computational chemistry [9], and biomedical image analysis [16]. Graph similarity computation, i.e. the problem to predict similarity between arbitrary pairs of graph-structured objects, is one of the

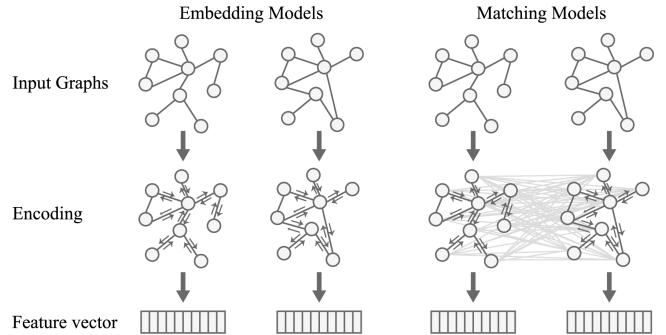


Figure 1: Two classes of existing data-driven models for graph similarity computation.

fundamental challenges and appears in various real-world applications, including biological molecular similarity search [15, 31] and social group network similarity identification [23, 30].

To compute graph-graph similarity, evaluation metrics such as Graph Edit Distance (GED) [27] were developed. Traditional methods for these metrics can be divided into two classes. The first one includes algorithms like [26] and [21] that calculate the exact values. While the exact similarity scores for sure help us better understand the relationship between graphs, the problem of exponential time complexity of exact graph similarity computation remains. The second class, which includes algorithms such as [22], [12], [7], [17] and [25], only computes the approximate values and saves time in return. However, these algorithms still run with polynomial or even sub-exponential time complexity.

With the rapid development of deep learning technology, graph neural networks (GNNs) which automatically extract the graph's structural characteristics provide a new solution for similarity computation of graph structures. Typically, GNN-based solution involves two stages: (1) embedding, which maps each graph to its representation feature vector, making similar graphs close in the vector space; (2) similarity computation based on these feature vectors. With different methods in the first stage, existing deep learning techniques for graph similarity computation can be classified into two categories, as illustrated in Fig. 1. The first category, exemplified by HIERARCHICALLY MEAN (GCN-MEAN) and HIERARCHICAL MAX (GCN-MAX) [5], directly maps graphs to feature vectors respectively by hierarchically coarsening the graphs and computes similarity based on the representation vectors of the two graphs. The second category embraced by GRAPH MATCHING NETWORKS (GMN) [19] embeds pair of graphs at the same time with cross-graph low-level interactions. Other methods like GSimCNN [3] and

*Equal contribution with order determined by rolling the dice.

GRAPHSIM [2] are similar to the second category except that they do not generate two separate feature vectors but instead directly embed graph pair to similarity score with cross-graph interactions. Meanwhile SIMGNN [1] deploy the two categories above parallelly. For simplicity, we call the first category embedding models and the second matching models in the rest of the paper.

In short, embedding models are efficient but not effective due to the lack of cross-graph fine-grained interactions and matching models are generally more effective but not efficient due to the low-level interactions across whole graphs. Let's take graph similarity search problem as an example for efficiency. Assume there are K graphs in the database and here comes a new graph. We want to compute the similarity score between this new graph with all the graphs in the database to find out the most similar graph with it. Because embedding models can embed all the graphs in the database to their own feature vectors in advance, these models only need to forward the new graph to its feature vector and compute similarity K times based on these feature vectors. Meanwhile, matching models have to forward the new graph respectively with all the graphs in the database (cross-graph interactions can not be finished in advance), which is time-consuming. Details about time complexity analysis will be shown in Section 4. However, as the generation process of feature vectors in embedding models do not involve interaction between graphs, the performance of embedding models is far worse than that of matching models.

[1], [3], [2] conduct their experiments of graph-graph similarity regression mostly on relatively small graphs, where there are only around 10 nodes in each graph, while [19] only consider graph-graph classification task. For large-scale graphs, it is difficult for embedding models to learn an embedding to express all the features while capturing subtle structural difference between two graphs, leading to a decline in accuracy. Meanwhile matching models will consume a lot of time due to the pairwise cross-graph interactions between nodes (at least quadratic time complexity over number of nodes), making them not easily scalable to large graphs. However, large-scale graphs (graph with hundreds of nodes) similarity computation is very important in domains such as Bio-informatics, Pattern Recognition, Social Network, etc. Thus in this paper, we focus on similarity computation problem on relatively large-scale graphs and propose our "embedding-coarsening-matching" graph similarity computation framework **CoSIM-GNN**, i.e., Coarsening-based Similarity Computation via Graph Neural Networks. As illustrated in Fig. 2, to better use the hierarchical nature of large-scale graphs, graph embedding layers and pooling layers are first applied to encode and coarsen the graphs. Then matching mechanism is deployed on the coarsened graph pair to compute similarity between graphs. In the first two stages of our model, there is no interaction across graphs so this part can be finished in advance in inference time or similarity search problem in order to save time. Meanwhile the intra-attention brought by coarsening and inter-attention introduced in matching part guarantee the performance, which is even better than directly applying the matching models in our experiments. This process is similar to large biological molecular identification process, where we always first transform the whole molecular to functional groups and identify the molecular based on these groups with denser local topology.

Many existing graph pooling methods can be incorporated into our framework and achieve relatively good performance. However, we notice that some state-of-the-art pooling mechanisms [14] involve generating centroids for cluster assignments, which never relies on the input graphs. This does not make sense intuitively because the centroids for different graphs should be different. Thus we propose a novel pooling layer **ADAPTIVE POOLING**. The generation process of centroids in **ADAPTIVE POOLING** is **input-related** and still keep the property of **permutation invariance**, leading to better performance than state-of-the-art pooling techniques. We highlight our main contributions as follows:

- We propose a novel framework, which first hierarchically encodes and coarsens graphs and then deploys a matching mechanism on the coarsened graph pairs, to address the challenging problem of similarity computation between large graphs.
- We propose a novel pooling operation **ADAPTIVE POOLING**. The generation of centroids in this layer is based on the input graph, which leads to better performance while maintaining permutation invariance.
- We create a set of synthetic datasets and collect a set of real-world datasets with different sizes for both graph-graph classification and similarity regression tasks which provides new benchmarks to study graph similarity computation.
- We conduct extensive experiments on real-world datasets and synthetic datasets consisting of large graphs. Our framework shows significant improvement in time complexity as compared to matching models. It also outperforms matching models (thus far better than embedding models) on similarity regression and classification tasks.
- Our framework is able to learn from graph pairs with a relatively small number of nodes (approximate 100) and then be deployed to infer similarity between huge graphs with thousands of nodes.

2 PRELIMINARIES

2.1 Problem Formulation of Graph Similarity Learning

Given a pair of graph inputs $(G^{(1)}, G^{(2)})$, the research goal of graph similarity computation in this paper is to produce a similarity score $y \in \mathcal{Y}$. The graph $G^{(1)}$ is represented as a set of $n_{in}^{(1)}$ nodes with a feature matrix $X_{in}^{(1)} \in \mathbb{R}^{n_{in}^{(1)} \times d_{in}^{(1)}}$ and an adjacency matrix $A_{in}^{(1)} \in \mathbb{R}^{n_{in}^{(1)} \times n_{in}^{(1)}}$. Similarly, the graph $G^{(2)}$ is represented as a set of $n_{in}^{(2)}$ nodes with a feature matrix $X_{in}^{(2)} \in \mathbb{R}^{n_{in}^{(2)} \times d_{in}^{(2)}}$ and an adjacency matrix $A_{in}^{(2)} \in \mathbb{R}^{n_{in}^{(2)} \times n_{in}^{(2)}}$.

When performing graph similarity prediction tasks, y is the similarity score $y \in (0, 1]$; when performing graph pair classification tasks, $y \in \{-1, 1\}$ indicates whether the graph pair is similar or not. The model is trained based on a set of training triplets of structured input pairs and scalar output scores $(G_1^{(1)}, G_1^{(2)}, y_1), (G_2^{(1)}, G_2^{(2)}, y_2), \dots, (G_N^{(1)}, G_N^{(2)}, y_N)$, where N is the size of training set.

2.2 Graph Similarity Computation

2.2.1 Graph Similarity Metrics.

Graph edit distance (GED) as a similarity measure is preferred over other distances or similarity

measures because of its generality and broad applicability [10]. The Graph Edit Distance (GED) is defined as the minimum cost taken to transform one graph to the other via a sequence graph edit operations. Here an edit operation on a graph is an insertion or deletion of a vertex/edge or relabelling of a vertex.

2.2.2 Traditional Algorithms. Various traditional heuristic methods have been proposed for approximation of graph similarity, including [22], [12], [7], [17] and [25]. These algorithms aim to reduce the time complexity with the sacrifice in accuracy. However, they always achieve an unsatisfactory trade-off between accuracy and efficiency.

2.2.3 Data-driven Methods. Data-driven methods can be classified into embedding models and matching models, and they have the key advantage of efficiency due to the nature of neural network computation. However, existing methods are still not easily scalable to large-scale graphs. Embedding models such as [5] are efficient but not effective due to the lack of cross-graph low-level interactions. Matching models such as [19], [3], [2] and [1], are generally effective but not efficient due to the need of low-level interactions across whole graphs.

2.3 Graph Pooling

In order to make our method efficient and easily scalable to large-scale graphs, we adopt graph pooling layers to coarsen original graphs and then deploy fine-grained cross-graph interactions on these coarsened (smaller and denser) graphs. Graph pooling (down-sampling) operations aim at reducing the number of graph nodes and learning new representations. DIFFPOOL [37] treats the graph pooling as a node clustering problem and trains two parallel GNNs to compute node representations and cluster assignments. GPOOL [8] and SAGPOOL [18] drop nodes from the original graph rather than group multiple nodes to form a cluster in the pooled graph. They devise a top-K node selection procedure to form an induced sub-graph for the next input layer. Although they are more efficient than DIFFPOOL, they do not aggregate nodes nor compute soft edge weights. This makes them unable to preserve node and edge information effectively. Based on DIFFPOOL, MEMPOOL [14] also learns soft cluster assignments, and uses a clustering-friendly distribution to compute the attention scores between nodes and clusters. However, MEMPOOL generates centroids (which are used to compute soft assignments) without involving the input graphs, which does not make sense intuitively because the centroids for different input graphs should be different. To address this limitation, we propose ADAPTIVE POOLING, which generates centroids that are input-related to graphs while keeping the property of permutation invariance.

3 PROPOSED FRAMEWORK

In order to reduce the high time consumption brought by low-level interaction across whole large graphs and take the advantage of the combination of intra- and inter- attention mechanism, we propose our novel CoSim-GNN framework, as shown in Fig. 2. In this section, we respectively introduce how each stage works in details. We use bold font for matrices and tilt font for function in this section. The right superscript of a matrix stands for graph number indicator and the right subscript stands for the stage of the matrix. For example,

$\mathbf{X}_{in}^{(1)}$ means the node feature matrix for the first input graph and $\mathbf{A}_{encode}^{(2)}$ means the adjacency matrices for the second graph after encoding.

Starting with two input node sets denoted as $\mathbf{X}_{in}^{(1)} \in \mathbb{R}^{n_{in}^{(1)} \times d_{in}^{(1)}}$ and $\mathbf{X}_{in}^{(2)} \in \mathbb{R}^{n_{in}^{(2)} \times d_{in}^{(2)}}$, as well as the adjacency matrix $\mathbf{A}_{in}^{(1)} \in \mathbb{R}^{n_{in}^{(1)} \times n_{in}^{(1)}}$ and $\mathbf{A}_{in}^{(2)} \in \mathbb{R}^{n_{in}^{(2)} \times n_{in}^{(2)}}$, we in each part first give the overall equation on how the stage works and then make detailed explanations on the overall equation.

3.1 Encoding

In the first stage, we employ k encoding layers (F_1, F_2, \dots, F_k) on the two input graphs respectively for embedding feature of nodes and transform the feature dimension of nodes to d_{encode} , just as shown in (1) below:

$$\mathbf{X}_{encode}^{(i)}, \mathbf{A}_{encode}^{(i)} = F_k(F_{k-1}(\dots F_1(\mathbf{X}_{in}^{(i)}, \mathbf{A}_{in}^{(i)}))) \quad (1)$$

where $i = 1, 2$, $\mathbf{X}_{encode}^{(i)} \in \mathbb{R}^{n_{in}^{(i)} \times d_{encode}}$, $\mathbf{A}_{encode}^{(i)} \in \mathbb{R}^{n_{in}^{(i)} \times n_{in}^{(i)}}$. (2) shows that F_j ($j = 1, 2, \dots, k$) is consisted of a graph convolution layer GC , a non-linear activation σ and a batchnorm layer bn .

$$F(\mathbf{X}, \mathbf{A}) = bn(\sigma(GC(\mathbf{X}, \mathbf{A}))) \quad (2)$$

We use ReLU for σ here and graph embedding layers GC can be GCN [5], GAT [33] or GIN [34].

3.2 Coarsening

What this stage does is to pool the encoded graphs, $\mathbf{X}_{encode}^{(i)}$ and $\mathbf{A}_{encode}^{(i)}$, to coarsened graphs, $\mathbf{X}_{pool}^{(i)} \in \mathbb{R}^{n_{pool} \times d_{pool}}$ and $\mathbf{A}_{pool}^{(i)} \in \mathbb{R}^{n_{pool} \times n_{pool}}$. The overall transformation is shown in equation 3, where σ is a non-linear activation function, $\mathbf{W} \in \mathbb{R}^{d_{encode} \times d_{pool}}$ is a trainable parameter matrix standing for a linear transformation and $\mathbf{C}^{(i)} \in \mathbb{R}^{n_{pool} \times n_{in}^{(i)}}$ is an assignment matrix representing a projection from the original node number to pooled node number. As $\mathbf{C}^{(i)}$ assigns weights for nodes in the input graph to nodes in the coarsened graph, it indeed stands for an intra-attention mechanism. Note here that because coarsening is done inside separate graph, we eliminate i in the following detailed explanations.

$$\begin{aligned} \mathbf{X}_{pool}^{(i)} &= \sigma(\mathbf{C}^{(i)} \mathbf{X}_{encode}^{(i)} \mathbf{W}) \\ \mathbf{A}_{pool}^{(i)} &= \sigma(\mathbf{C}^{(i)} \mathbf{A}_{encode}^{(i)} (\mathbf{C}^{(i)})^\top) \end{aligned} \quad (3)$$

Different approaches are adopted to compute the assignment matrix \mathbf{C} in different pooling layers. When we look at one of the most representative pooling layers so far, MEMPOOL [14], we notice that it generates memory heads, which stands for the new centroids in the space of pooled graphs, without the involvement of the input graph. However, intuitively, the new centroids for different graphs should be different. Thus here we propose a new method: ADAPTIVE POOLING, to calculate \mathbf{C} . Inspired by the multi-head attention mechanism [32] which can increase the representation capacity, we first generate h batches of centroids $\mathbf{K} \in \mathbb{R}^{h \times n_{pool} \times d_{encode}}$ based on the encoded graph (**permutation invariance** remains) and then compute and aggregate the relationship between every batch of centroids and the encoded graph, leading to the final assignment

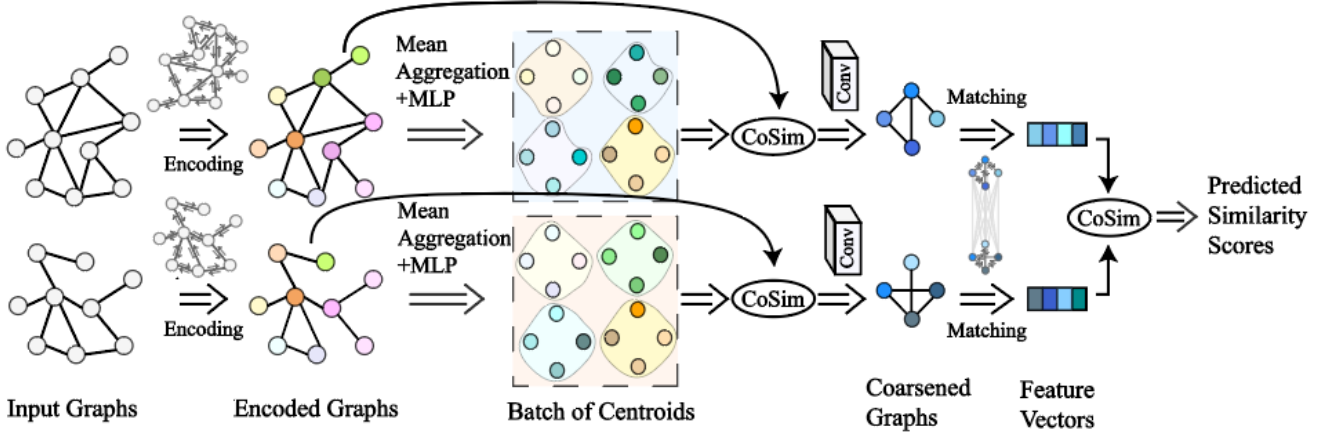


Figure 2: An overview of our "embedding-coarsening-matching" framework CoSim-GNN. The encoding part aggregates features, respectively, inside the two graphs. The coarsening stage then transforms the encoded graphs into batches of centroids, and these centroids jointly coarsen the graphs. Finally, matching-based feature aggregation is deployed on the coarsened graph pair, and the similarity score is computed based on the two graph-level feature vectors.

matrix C . Detailed ablation study about pooling layers is conducted in Section 5, which demonstrates the effectiveness of ADAPTIVE POOLING.

As shown in equation 4, an average aggregation F_{avg} over the encoded graph is deployed, transforming $X_{encode} \in \mathbb{R}^{n_{in} \times d_{encode}}$ to $X_{avg} \in \mathbb{R}^{1 \times d_{encode}}$. Then an Multiple Layer Perceptron (MLP) is applied to map X_{avg} to $K \in \mathbb{R}^{(h \times n_{pool}) \times d_{encode}}$, after which K is reshaped to $\mathbb{R}^{h \times n_{pool} \times d_{encode}}$. Note that the generation of batches of centroids here is dependent on the encoded graph (input of this layer), which makes sense because centroids for different input graphs in the training and testing set should be different. Besides, due to the mean aggregation, we keep the permutation invariance property in our proposed pooling method, one of the most important properties for graph-related deep learning architecture.

$$K = MLP(F_{avg}(X_{encode})) \quad (4)$$

Then we compute the relationship $C_p \in \mathbb{R}^{n_{pool} \times n_{in}}$ ($p = 1, 2, \dots, h$) between every batch of centroids $K_p \in \mathbb{R}^{n_{pool} \times d_{encode}}$ ($p = 1, 2, \dots, h$) and $X_{encode} \in \mathbb{R}^{n_{encode} \times d_{encode}}$. A simple cosine similarity is deployed here and leads to satisfactory pooling performance, as described in equation 5, where a row normalization is deployed in the resulting similarity matrix.

$$\begin{aligned} C_p &= \text{cosine}(K_p, X_{encode}) \\ C_p &= \text{normalize}(C_p) \end{aligned} \quad (5)$$

We finally aggregate the information of h relationship $C_p \in \mathbb{R}^{n_{pool} \times n_{in}}$. In (6), we concatenate the centroids of h groups C_p ($p = 1, 2, \dots, h$) and a learnable weighted sum Γ_ϕ is deployed on the first dimension,

resulting in the assignment matrix C .

$$C = \Gamma_\phi \begin{pmatrix} |h| \\ p=1 \end{pmatrix} C_p \quad (6)$$

3.3 Matching

As shown in (7), this part aims to compute similarity based on the interaction of two coarsened graphs. f_{match} takes the two coarsened graphs as input and generates feature vectors $X_{final}^{(i)}$ for respective graph. Note that i and j in the first equation in (7) indicate two different graphs in the graph pair, that is when $i = 1, j = 2$ and when $i = 2, j = 1$. Then a cosine similarity is deployed for the similarity score. Finally we compute the Mean Squared Loss between the score and the ground truth similarity GT for backward update.

$$\begin{aligned} X_{final}^{(i)} &= f_{match}(X_{pool}^{(i)}, A_{pool}^{(i)}, X_{pool}^{(j)}, A_{pool}^{(j)}) \\ \text{Score} &= \text{cosine}(X_{final}^{(1)}, X_{final}^{(2)}) \\ \text{Loss} &= \frac{1}{batchsize} \sum_{i=1}^{batchsize} (Score(i) - GT(i))^2 \end{aligned} \quad (7)$$

Several matching mechanisms such as GSIMCNN [3] and GMN [19], can be deployed for f_{match} and here we give a simple example. As shown in (8), there are several propagators f_P and one aggregator f_A to transform the pooled graphs to respective feature vectors with cross-graph interactions. Note here that we will eliminate the subscript $pool$ of matrix X and A in the following detailed explanations.

$$X_{final}^{(i)} = f_A(f_P \dots (f_P(X_{pool}^{(i)}, A_{pool}^{(i)}, X_{pool}^{(j)}, A_{pool}^{(j)}))) \quad (8)$$

In the propagators f_p , we aggregate both inside features ($I^{(i)}$) and external features ($M^{(i)}$). As shown in (9), we first propagate features inside respective graph with a GAT [33] and add up the features for all the neighbors of every node to form $I^{(i)} \in \mathbb{R}^{n_{pool} \times d_{pool}}$.

$$X_{gat}^{(i)} = \text{GAT}\left(X^{(i)}, A^{(i)}\right) \quad (9)$$

$$I^{(i)}(k) = \sum_{\forall j, A^{(i)}(k, m) \neq 0} X_{gat}^{(i)}(m), \quad k = 1, 2, \dots, n_{pool}$$

As for the inter-attention, we compute $M^{(i)} \in \mathbb{R}^{n_{pool} \times d_{pool}}$ with f_{cross} in (10). First a relationship mask is generated across the graph pair, which involves matrix multiply for the normalized graphs and a softmax activation (σ). Then the interaction between the two coarsened graphs is realized by applying the mask to the graph X^i and subtracting X^i with the masked X^j .

$$M^{(i)} = f_{cross}\left(X^{(i)}, X^{(j)}\right) \quad (10)$$

$$= X^{(i)} - \sigma\left(\frac{X^{(i)}}{\|X^{(i)}\|_{L2}} \cdot \frac{(X^{(j)})^\top}{\|X^{(j)}\|_{L2}}\right) \cdot X^{(j)}$$

After the above two steps, we apply f_{node} to embrace all these features including the original input by concatenating all these features and deploying an MLP on the concatenated matrix.

$$X_P^{(i)} = f_{node}\left(X^{(i)}, I^{(i)}, M^{(i)}\right) \quad (11)$$

$$= \text{MLP}\left(\|X^{(i)}, I^{(i)}, M^{(i)}\|\right)$$

As for the aggregator, we use the following module proposed in (Li et al., 2015), where L_G , L_{gate} and L are simply implemented with Multiple Layer Perceptron and the nonlinear activation σ is the softmax function.

$$X_{final}^{(i)} = f_A\left(X_P^{(i)}\right) \quad (12)$$

$$= L_G\left(\sigma\left(L_{gate}\left(X_P^{(i)}\right)\right) \cdot L\left(X_P^{(i)}\right)\right)$$

4 TIME COMPLEXITY ANALYSIS IN GRAPH SIMILARITY SEARCH PROBLEM

For a pair of input graphs $X_{in}^{(1)} \in \mathbb{R}^{n_{in}^{(1)} \times d_{in}^{(1)}}$ and $X_{in}^{(2)} \in \mathbb{R}^{n_{in}^{(2)} \times d_{in}^{(2)}}$, we can assume that they separately have $m^{(1)}$, $m^{(2)}$ edges and the final embedded feature vectors for both graphs are $X_{final}^{(1)} \in \mathbb{R}^{d_{final}}$ and $X_{final}^{(2)} \in \mathbb{R}^{d_{final}}$. Then we can analyse the time complexity over $n_{in}^{(i)}$, $m^{(i)}$ and d_{final} . Note that due to the fact that there exists a lot of variance for each model, we here analyse the simplest cases for each category and the real time consumption will be presented later in the Section 5. Table 1 shows the time complexity comparison for embedding models, matching models and our proposed framework, which will be discussed in details in the three parts below. In our settings, n_{pool} is far less than n , thus our framework costs far less time than matching models do, especially when the node number of the graphs is very large.

4.1 Embedding models

Considering the simplest case here for embedding models, we only visit every edge once and deploy two computational operational on the two nodes it connect, which contributes to the feature of local topology. Thus the computation complexity for these cases is $O(2 \times m^{(i)})$, $i = 1, 2$.

4.2 Matching models

Assuming the simplest case here for matching models, we first compute the relationship across $X_{in}^{(1)}$ and $X_{in}^{(2)}$. This part involves $n_{in}^{(1)} \times n_{in}^{(2)}$ computational operations because we have to calculate the connection between every node in $X_{in}^{(1)}$ to all nodes in $X_{in}^{(2)}$. Then for each input graph, we also visit every edge once and deploy two computational operational on the two nodes it connect, which also makes contribution to the feature of local topology. Thus the computation complexity for these cases is $O(2 \times m^{(i)} + n_{in}^{(1)} \times n_{in}^{(2)})$, $i = 1, 2$.

4.3 Our framework

For our framework, we take the denotation in Section 3, that is the number of nodes in coarsened graphs is n_{pool} . In the embedding stage, we similarly have to visit every edge once and compute twice. Then in the pooling part, we make an transformation from $n_{in}^{(i)}$ dimensional space to n_{pool} dimensional space, which costs us $n_{in}^{(i)} \times n_{pool}$ computational operations. Finally in the matching stage, like what have been analysed in the previous section, we need $2 \times m_{pool}^{(i)} + n_{pool} \times n_{pool}$, $i = 1, 2$ operations. Thus the resulting complexity is $O(2 \times m^{(i)} + n_{in}^{(i)} \times n_{pool} + 2 \times m_{pool}^{(i)} + n_{pool} \times n_{pool})$, $i = 1, 2$.

5 EXPERIMENTS AND RESULTS

5.1 Data Preparation

Some of the existing graph datasets used in graph similarity computation, such as AIDS and LINUX (after filtering in [1]), the number of nodes is relatively small in each graph. Thus the characteristics of the entire graphs can be easily characterized and there is no need to coarsen the graphs for better similarity computation results. From this point of view, we use the following four real-world datasets and four synthetic datasets for the experiments. Statistics of datasets are presented in Appendix C. We deploy the same method as that in [1] and randomly divide each dataset to three sub-sets containing 60%, 20% and 20% of all graphs for training, validating and testing.

5.1.1 Real-world Datasets.

- **IMDB** [36]: IMDB dataset contains more than one thousand graphs indicating appearance of movie actors/actresses in the same movie. We filter the original dataset and choose all the graphs that have 15 or more nodes for experiments.
- **Enzymes** [28]: The Enzymes dataset consists of various types of enzymes and the least node number is 30, which is suitable for our setting.
- **COIL** [24]: We follow the same settings as that in [19], and treat graphs in the same class as similar.

Table 1: Time complexity comparison in similarity search problem.

Categories	Time Complexity
Embedding models	$O(2 \times m + K \times d_{final})$
Matching models	$O((2 \times m \times 2 + n \times n + d_{final}) \times K)$
CoSim-GNN	$O(2 \times m + n \times n_{pool} + (2 \times m_{pool} \times 2 + n_{pool} \times n_{pool} + d_{final}) \times K)$

- **OpenSSL** [35]: The OpenSSL dataset was built and released for binary code similarity detection with prepared 6 block-level numeric features.

We use the first two real-world datasets for similarity regression task and the last two for similarity classification task.

5.1.2 Synthetic Datasets. Main advantages of creating and using synthetic datasets are as follows:

- With synthetic datasets, we can obtain more accurate similarity labels (ground truth similarities). Detail reasons are presented in Appendix E.
- Synthetic datasets allow us to perform more controllable experiments for studying the effect of graph size on different models, which help us better understand strengths and weakness of different models.

To generate a synthetic dataset, we need to generate graphs and give ground truth similarity for graph pairs. A small number of basic graphs is first generated and then we prune the basic graphs to generate derived graphs with two different categories of pruning rules: BA model [11] and ER model [6][4]. Details about why we adopt this process and how these two models work will be presented in Appendix B. We generate 4 datasets: **BA-60**, **BA-100**, **BA-200** and **ER-100**, where the first two characters stand for generation rule and behind is the number of nodes in the basic graphs for that dataset. These datasets provide new benchmarks to study graph-graph similarity computation. Details and reasons of why we currently do not create datasets with even larger graphs are also presented in Appendix E.

5.1.3 Ground Truth Similarity Generation. To calculate the GED ground truth values of graph pairs, we deploy the same mechanism as that in [1]. Since all the approximate GED algorithms return an upper bound of the exact GED value, they used the minimum GED returned by all approximate GED algorithms for each pair of graph as the ground truth GED. Then with ground truth GED, we can easily get the ground truth similarity. For synthetic datasets, we use the minimum value among four evaluation indicators: the three values calculate respectively by HUNGARIAN, VJ, and BEAM and the GED value we obtain while generating the graph (detailed in Section 5.1.4). For real-world datasets, we used the minimum value returned by these three algorithms as the ground truth GED. Then we convert this ground truth GED value to the ground truth similarity score with a normalization of the GED followed by a exponential function, resulting in a value among [0, 1].

$$nGED(G_1, G_2) = \frac{GED(G_1, G_2)}{(|G_1| + |G_2|)/2} \quad (13)$$

$$f(x) = e^{-x}$$

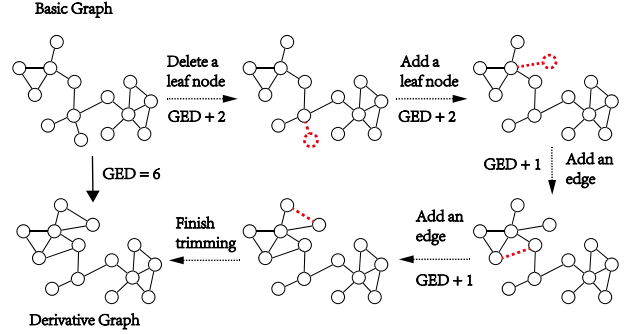


Figure 3: Generate a derivative graph with a GED of 6 from the basic graph. It is not necessary to use all three methods in real trimming. Here is only one case.

where $|G_i|$ represents the total number of nodes in graph G_i . It is worth noting that the neural network approach can learn graph similarity from all the data (similarity value) generated by different traditional algorithmic approaches, thus has the potential to be more effective than any traditional graph similarity computation algorithm.

5.1.4 Ground Truth Generation for Synthetic Datasets. Here we mainly discuss details about the GED value obtained when converting basic graphs to derived ones. As shown in Fig. 3, when generating a derivative graph with a specific GED from the basic graph, we randomly select among the above three methods (randomly delete a leaf node, add a leaf node or add an edge) to generate a set of operations, and the sum of GED accumulated by all operations is the exact GED value. As proposed formerly, we then take the minimum value of the trimming GED and the calculated GED with the three algorithms as the final ground truth GED value.

5.2 Experiment Settings

5.2.1 Evaluation Metrics. We apply six metrics to evaluate all the models: *TIME*, *Mean Squared Error (MSE)*, *Mean Absolute Error (MAE)*, *Spearman's Rank Correlation Coefficient (ρ)* [29], *Kendall's Rank Correlation Coefficient (τ)* [13] and *Precision at k ($p@k$)*. *TIME* is the least average time a model need to compute similarity over one graph pair with the strategy similar to what we discuss in Section 4. *MSE* and *MAE* measure the average squared/absolute

Table 2: Results for MSE and MAE in 10^{-3} . The three traditional method are involved in the ground truth computation and thus these values are labeled with superscript *.

Method	BA-60		BA-100		BA-200		ER-100		IMDB		Enzymes	
	MSE	MAE	MSE	MAE								
HUNGARIAN	186.19*	332.20*	205.38*	343.83*	259.06*	379.38*	236.15*	421.66*	2.67*	16.60*	4.67*	60.70*
VJ	258.73*	294.83*	273.94*	404.61*	314.45*	426.86*	275.22*	463.53*	7.68*	22.73*	19.14*	76.86*
BEAM	59.14*	129.26*	114.02*	206.76*	186.03*	287.88*	104.73*	226.42*	0.39*	3.93*	2.97×10^{-5} *	4.43×10^{-3} *
GCN-MEAN	5.85	53.92	12.53	90.88	23.66	127.82	16.58	92.98	22.17	55.35	10.69	61.09
GCN-MAX	13.66	91.38	3.14	42.24	22.77	107.58	79.09	211.07	47.14	123.16	13.15	67.64
SimGNN	8.57	63.80	6.23	47.80	3.06	32.77	6.37	45.30	7.42	33.74	13.96	49.04
GSIMCNN	5.97	56.05	1.86	30.18	2.35	32.64	2.93	34.41	5.01	30.43	2.48	26.79
GMN	2.82	38.38	4.14	34.17	1.16	26.60	1.59	28.68	3.82	27.28	3.02	35.86
CoSIM-CNN	2.50	35.53	1.49	27.20	0.53	18.44	2.78	33.36	10.37	38.03	24.64	104.05
CoSIM-ATT	2.04	33.41	0.97	22.95	0.73	16.26	1.39	27.27	1.53	16.57	1.48	25.95
CoSIM-SAG	3.26	38.85	3.30	33.14	1.91	35.48	1.55	29.84	1.62	16.08	1.33	28.19
CoSIM-TopK	3.44	40.87	1.24	25.61	0.88	20.63	2.04	34.28	1.98	20.02	1.99	28.95
CoSIM-MEM	5.45	48.07	1.11	24.59	0.32	14.82	1.74	26.78	1.57	17.02	1.21	26.22
CoSIM-GNN10	2.04	33.04	1.01	23.53	0.40	16.43	1.38	27.43	1.68	17.57	1.38	24.73
CoSIM-GNN1	1.84	32.36	0.95	22.06	0.36	15.42	1.17	25.73	2.00	18.62	1.09	25.88

difference between the predicted similarities and the ground-truth similarities. Details and results about τ , ρ and $p@k$ will be shown in the Appendix A.

5.2.2 Baseline Methods. There are three types of baselines. The first category consists of traditional methods for GED computation, where we include *A*-Beamsearch (Beam)* [22], *Hungarian* [17] [25], and *Vj* [12] [7]. *Beam* is one of the variants of *A** algorithm and its time complexity is sub-exponential. *Hungarian* based on the Hungarian Algorithm for bipartite graph matching, and *Vj* based on the Volgenant and Jonker algorithm, are two algorithms in cubic-time. The second category is made up of embedding models, including *GCN-Mean* and *GCN-Max* [5]. The third category consists of matching models and we here involve *GMN* [19] and two matching-based models: *SimGNN* [1] and *GSIMCNN* [3].

5.2.3 Settings in Our Proposed Framework. We provide experiments on seven kinds of variants of our framework to demonstrate its scalability and the effectiveness of *ADAPTIVE POOLING*. The names and settings of these seven variants are shown in Table 3. The parameters in our framework are as below: $k = 3$, $n_{encode} = 64$ (same in baselines), $h = 5$, $m = 5$, $l_{ins} = 2$, $l_{node} = 2$, $batchsize = 128$ (same in baselines).

We train models for 2000 iterations on BA- and Enzymes datasets, 5000 iterations on IMDB and 10000 iterations on ER-. The model that performs the best on validation sets is selected for testing. Experiments are conducted on the same device and details about this device are in Appendix D.

5.3 Results and Analysis

5.3.1 Effectiveness and Efficiency. Statistic results are shown respectively in Table 2 and 4. For better understanding the results, we highlight best MSE and MAE results among all the models in Table 2 and highlight the least time consumption respectively among the

Table 3: Settings of different models in our framework.

Model Names	Embedding	Coarsening	Matching
CoSIM-ATT	GIN	SIMATT [1] ($n_{pool} = 1$)	OURMATCH
CoSIM-CNN	GIN	ADAPTIVEPOOL ($n_{pool} = 10$)	GSIMCNN [3]
CoSIM-SAG	GIN	SAGPOOL [18] ($n_{pool} = 10$)	OURMATCH
CoSIM-TopK	GIN	TOPKPOOL [8] ($n_{pool} = 10$)	OURMATCH
CoSIM-MEM	GIN	MEMPOOL [14] ($n_{pool} = 10$)	OURMATCH
CoSIM-GNN10	GIN	ADAPTIVEPOOL ($n_{pool} = 10$)	OURMATCH
CoSIM-GNN1	GIN	ADAPTIVEPOOL ($n_{pool} = 1$)	OURMATCH

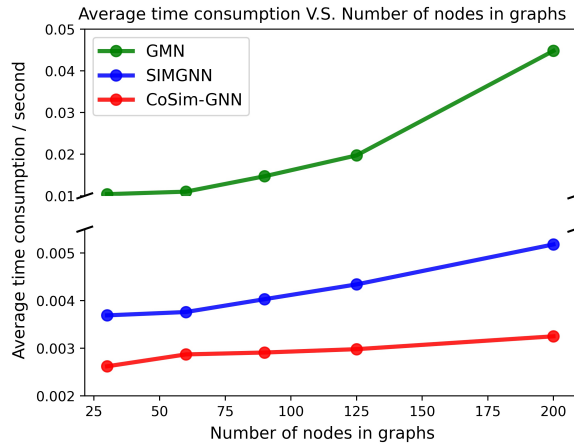
four different categories (traditional methods, embedding models, matching models and our proposed models) in Table 4. It is shown in the statistic that models in our framework outperform matching models in every dataset and our proposed pooling layer achieves the best performance among all the tested pooling method. Here we emphasize three aspects. Firstly, it can be found that for all the datasets, our framework outperforms all the traditional methods, embedding models and matching models on both MSE and DEV . Secondly, it is shown that our CoSIM-GNN1 runs faster than any matching model. When we take comparisons among BA datasets, it is clear that our time consumption keeps low as the node number increases and the gaps on time consumption between our models and matching models keep increasing. Especially when we look at CoSIM-GNN1 and GMN, our model requires **1/3**, **1/5**, **1/14**, **1/5**, **1/5** and **1/5** as the time consumption of GMN respectively on BA-60, BA-100, BA-200, ER-100, IMDB and Enzymes. Thirdly, when we look at the results among all the models under our framework, it can be found that in 4 out of the all 6 datasets, our pooling layer performs better than all other pooling layers, which demonstrates the effectiveness of our proposed pooling layer.

We also select graphs with different number of nodes and run GMN, SimGNN and CoSIM-GNN for over 100 times. Average time

Table 4: Results for average time consumption on one pair of graphs in milliseconds.

Method	BA-60	BA-100	BA-200	ER-100	IMDB	ENZYMEs
HUNGARIAN	>100	>100	>100	>100	>100	>100
VJ	>100	>100	>100	>100	>100	>100
BEAM	>100	>100	>100	>100	>100	>100
GCN-MEAN	1.31	1.48	1.79	1.51	1.68	1.08
GCN-MAX	1.32	1.46	1.85	1.49	1.58	1.25
SIMGNN	2.92	3.24	5.26	3.46	4.34	2.62
GSIMCNN	2.07	2.73	5.16	2.86	3.16	2.08
GMN	5.77	9.36	28.57	10.00	9.89	7.65
CoSIM-CNN	1.99	2.16	2.67	2.19	2.21	1.98
CoSIM-ATT	1.85	2.02	2.34	1.99	2.12	1.85
CoSIM-SAG	2.18	2.59	3.97	2.65	2.33	1.92
CoSIM-TopK	2.08	2.28	2.51	2.28	2.83	1.91
CoSIM-MEM	3.30	3.56	3.95	3.50	3.58	3.48
CoSIM-GNN10	3.29	3.51	4.03	3.63	3.09	3.04
CoSIM-GNN1	1.83	2.01	2.31	1.97	2.08	1.82

consumption is shown in Figure 4. It can be found that as the average graph size increases, the time consumption of matching models grow much faster than our model's. The reason is that, theoretically, low-level cross-graph interactions in matching models need at least quadratic time complexity over number of nodes of the two graphs, which causes them not easily scalable to large graphs.

**Figure 4: Models' running time on different size of graphs.**

5.3.2 Generalization. Sometimes, due to the limitation of computing resources, we may not be able to train models on very large graph datasets (graphs that have thousands of nodes) efficiently. Therefore, it's interesting and meaningful to explore whether our model can be efficiently trained on small graph dataset and then be effectively applied to infer similarity on large graph pairs.

In this paper, we derive two sub-networks from the academic network of AMiner¹. The first sub-network includes 1,397 authors

¹<https://aminer.org/aminernetwork>

and 1446 edges representing the coauthor relationship and the second sub-network includes 1324 papers and 1977 edges representing the citation relationship. We use these two as the basic graphs, and then use the previously mentioned trimming method (the trimming steps are 10, 20, ..., 100), to get 198 trimming graphs, which with the two basic graphs constitute our Aminer dataset. Experimental results are in Table 5. In our experiments, GMN [19] can not be deployed to this dataset even with a 32GB RAM (error in memory overflow). It is found that CoSim-GNN outperform the other techniques in both MSE and MAE on the different dataset where graphs have much more nodes. Also the time consumption of CoSim-GNN is even lower than embedding models. This results are very promising in many other application including analysis on social network and very large biological molecular.

Table 5: Results on Aminer dataset to show models' generalization ability. MSE and MAE are in 10^{-3} and time is in second.

Method	GCN-MAX	GCN-MEAN	GSIMCNN	CoSIM-GNN
MSE	7.76	8.43	48.37	3.64
MAE	59.79	73.45	176.44	50.37
Time	6.72	6.96	32.00	6.46

5.4 Study of the Matching Layer

We conduct an ablation study on BA-100 dataset to validate the key components that contribute to the improvement of our CoSIM-GNN.

We focus on equation (11) and select different combination of X, I and M in the concatenation operation. Results are shown in Table 6. We can see that after removing X or I or M from CoSIM-GNN, the performance will drop, which proves that all modules are useful for similarity computation. What's more, it can be seen that if M is removed from the framework, the performance will drop the most. The conclusion here is that all the modules contributed to the framework and the main contribution is brought by M, which stands for cross-graph inter-attention.

Table 6: Ablation study in matching part.

	X&I&M	X&M	M	X&I
MSE	0.95	1.02	1.11	2.56
MAE	22.06	23.49	23.76	38.19

5.5 Graph-graph Similarity Classification

We conduct similarity classification experiments (classify graph pairs to “similar” or “dissimilar”) on three synthetic datasets we generate and two real benchmark datasets: OpenSSL [35] and COIL-DEL (COIL [24]). In Table 7, it can be found that “CoSim” models achieve the best performance on both synthetic and real datasets in classification task. Experiments also show that more pooling layers lead to better GED regression performance only when the node numbers of graphs are large, i.e. on the BA-200 dataset, and here we only use one coarsening layer for all graph classification tasks.

Table 7: Accuracy on classification task in %.

Method	BA-60	BA-100	BA-200	OpenSSL	COIL
GCN-Mean	92.56	91.43	91.38	78.93	73.94
GCN-Max	92.19	91.38	90.94	80.72	72.10
GSimCNN	93.78	98.75	98.94	89.50	80.44
CoSim-Mem	93.22	95.00	99.63	90.45	83.85
CoSim-GNN	97.50	99.38	99.75	94.66	88.30

6 CONCLUSION

In this paper, we propose CoSIM-GNN for efficient large-scale graph similarity computation, including three stages: encoding, coarsening and matching. Noticing that the generation of centroids for cluster assignments does not rely on the input graphs among current state-of-the-art graph pooling methods, we design a novel pooling method ADAPTIVE POOLING. Thorough experiments are conducted on various baselines, datasets and evaluation metrics to demonstrate the scalability, effectiveness and efficiency of CoSIM-GNN as well as the effectiveness of ADAPTIVE POOLING.

CoSIM-GNN opens up the door for learning large-scale graph similarity and the future focus will be on more efficient pooling and matching mechanisms, which are able to further improve the large graph similarity regression and classification in this novel framework. In addition, since obtaining sufficient similarity labels of relatively large-scale graphs is quite hard, it's also promising to explore self-supervised learning methods [20] for graph-graph similarity approximation.

REFERENCES

- [1] Yunsheng Bai, Hao Ding, Song Bian, Ting Chen, Yizhou Sun, and Wei Wang. 2018. SimGNN: A Neural Network Approach to Fast Graph Similarity Computation. *arXiv:1808.05689 [cs.LG]*
- [2] Yunsheng Bai, Hao Ding, Ken Gu, Yizhou Sun, and Wei Wang. [n.d.]. Learning-based Efficient Graph Similarity Computation via Multi-Scale Convolutional Set Matching.
- [3] Yunsheng Bai, Hao Ding, Yizhou Sun, and Wei Wang. 2018. Convolutional set matching for graph similarity. *arXiv preprint arXiv:1810.10866* (2018).
- [4] Béla Bollobás and Bollobás Béla. 2001. *Random graphs*. Number 73. Cambridge university press.
- [5] Michaël Defferrard, Xavier Bresson, and Pierre Vandergheynst. 2016. Convolutional Neural Networks on Graphs with Fast Localized Spectral Filtering. In *Advances in Neural Information Processing Systems 29*, D. D. Lee, M. Sugiyama, U. V. Luxburg, I. Guyon, and R. Garnett (Eds.). Curran Associates, Inc., 3844–3852. <http://papers.nips.cc/paper/6081-convolutional-neural-networks-on-graphs-with-fast-localized-spectral-filtering.pdf>
- [6] Paul Erdos. 1959. On random graphs. *Publicationes mathematicae* 6 (1959), 290–297.
- [7] Stefan Fankhauser, Kaspar Riesen, and Horst Bunke. 2011. Speeding Up Graph Edit Distance Computation through Fast Bipartite Matching. In *Graph-Based Representations in Pattern Recognition*, Xiaoyi Jiang, Miquel Ferrer, and Andrea Torsello (Eds.). Springer Berlin Heidelberg, Berlin, Heidelberg, 102–111.
- [8] Hongyang Gao and Shuiwang Ji. 2019. Graph U-Nets. *arXiv:1905.05178 [cs.LG]*
- [9] Justin Gilmer, Samuel S. Schoenholz, Patrick F. Riley, Oriol Vinyals, and George E. Dahl. 2017. Neural Message Passing for Quantum Chemistry. *arXiv:1704.01212 [cs.LG]*
- [10] Karam Gouda and Mosab Hassaan. 2016. CSI_GED: An efficient approach for graph edit similarity computation. In *2016 IEEE 32nd International Conference on Data Engineering (ICDE)*. IEEE, 265–276.
- [11] Hawoong Jeong, Zoltan Néda, and Albert-László Barabási. 2003. Measuring preferential attachment in evolving networks. *EPL (Europhysics Letters)* 61, 4 (2003), 567.
- [12] Roy Jonker and Anton Volgenant. 1987. A shortest augmenting path algorithm for dense and sparse linear assignment problems. *Computing* 38, 4 (1987), 325–340.
- [13] Maurice G Kendall. 1938. A new measure of rank correlation. *Biometrika* 30, 1/2 (1938), 81–93.
- [14] Amir Hosein Khasahmadi, Kaveh Hassani, Parsa Moradi, Leo Lee, and Quaid Morris. 2020. Memory-Based Graph Networks. In *International Conference on Learning Representations*. <https://openreview.net/forum?id=r1laNeBYPB>
- [15] Hans-Peter Kriegel, Martin Pfeifle, and Stefan Schönauer. 2004. Similarity Search in Biological and Engineering Databases. *IEEE Data Eng. Bull.* 27, 4 (2004), 37–44.
- [16] Sofia Ira Ktena, Sarah Parisot, Enzo Ferrante, Martin Rajchl, Matthew Lee, Ben Glocker, and Daniel Rueckert. 2017. Distance Metric Learning using Graph Convolutional Networks: Application to Functional Brain Networks. *arXiv:1703.02161 [cs.CV]*
- [17] Harold W Kuhn. 1955. The Hungarian method for the assignment problem. *Naval research logistics quarterly* 2, 1-2 (1955), 83–97.
- [18] Junhyun Lee, Inyeop Lee, and Jaewoo Kang. 2019. Self-attention graph pooling. *arXiv preprint arXiv:1904.08082* (2019).
- [19] Yujia Li, Chenjie Gu, Thomas Dullien, Oriol Vinyals, and Pushmeet Kohli. 2019. Graph Matching Networks for Learning the Similarity of Graph Structured Objects. *arXiv:1904.12787 [cs.LG]*
- [20] Xia Liu, Fanjin Zhang, Zhenyu Hou, Zhaoyu Wang, Li Mian, Jing Zhang, and Jie Tang. 2020. Self-supervised learning: Generative or contrastive. *arXiv preprint arXiv:2006.08218* 1, 2 (2020).
- [21] Ciaran McCreesh, Patrick Prosser, and James Trimble. 2017. A partitioning algorithm for maximum common subgraph problems. (2017).
- [22] Michel Neuhaus, Kaspar Riesen, and Horst Bunke. 2006. Fast Suboptimal Algorithms for the Computation of Graph Edit Distance. In *Structural, Syntactic, and Statistical Pattern Recognition*, Dit-Yan Yeung, James T. Kwok, Ana Fred, Fabio Roli, and Dick de Ridder (Eds.). Springer Berlin Heidelberg, Berlin, Heidelberg, 163–172.
- [23] Kirk Ogaard, Heather Roy, Sue Kase, Rakesh Nagi, Kedar Sambhoos, and Moises Sudit. 2013. Discovering patterns in social networks with graph matching algorithms. In *International Conference on Social Computing, Behavioral-Cultural Modeling, and Prediction*. Springer, 341–349.
- [24] Kaspar Riesen and Horst Bunke. 2008. IAM graph database repository for graph based pattern recognition and machine learning. In *Joint IAPR International Workshops on Statistical Techniques in Pattern Recognition (SPR) and Structural and Syntactic Pattern Recognition (SSPR)*. Springer, 287–297.
- [25] Kaspar Riesen and Horst Bunke. 2009. Approximate graph edit distance computation by means of bipartite graph matching. *Image and Vision computing* 27, 7 (2009), 950–959.
- [26] Kaspar Riesen, Sandro Emmenegger, and Horst Bunke. 2013. A novel software toolkit for graph edit distance computation. In *International Workshop on Graph-Based Representations in Pattern Recognition*. Springer, 142–151.
- [27] A. Sanfeliu and K. Fu. 1983. A distance measure between attributed relational graphs for pattern recognition. *IEEE Transactions on Systems, Man, and Cybernetics SMC-13*, 3 (1983), 353–362.
- [28] Ida Schomburg, Antje Chang, Christian Ebeling, Marion Gremse, Christian Heldt, Gregor Huhn, and Dietmar Schomburg. 2004. BRENDA, the enzyme database: updates and major new developments. *Nucleic acids research* 32, suppl_1 (2004), D431–D433.
- [29] Charles Spearman. 1961. The proof and measurement of association between two things. (1961).
- [30] Karsten Steinhaeuser and Nitesh V Chawla. 2008. Community detection in a large real-world social network. In *Social computing, behavioral modeling, and prediction*. Springer, 168–175.
- [31] Yuanyuan Tian, Richard C Mceachin, Carlos Santos, David J States, and Jignesh M Patel. 2007. SAGA: a subgraph matching tool for biological graphs. *Bioinformatics* 23, 2 (2007), 232–239.
- [32] Ashish Vaswani, Noam Shazeer, Niki Parmar, Jakob Uszkoreit, Llion Jones, Aidan N Gomez, Łukasz Kaiser, and Illia Polosukhin. 2017. Attention is all you need. In *Advances in neural information processing systems*, 5998–6008.
- [33] Petar Veličković, Guillem Cucurull, Arantxa Casanova, Adriana Romero, Pietro Lio, and Yoshua Bengio. 2017. Graph attention networks. *arXiv preprint arXiv:1710.10903* (2017).
- [34] Keyulu Xu, Weihua Hu, Jure Leskovec, and Stefanie Jegelka. 2018. How Powerful are Graph Neural Networks? *ArXiv abs/1810.00826* (2018).
- [35] Xiaojun Xu, Chang Liu, Qian Feng, Heng Yin, Le Song, and Dawn Song. 2017. Neural network-based graph embedding for cross-platform binary code similarity detection. In *Proceedings of the 2017 ACM SIGSAC Conference on Computer and Communications Security*. 363–376.
- [36] Pinar Yanardag and SVN Vishwanathan. 2015. Deep graph kernels. In *Proceedings of the 21th ACM SIGKDD International Conference on Knowledge Discovery and Data Mining*. 1365–1374.
- [37] Rex Ying, Jiaxuan You, Christopher Morris, Xiang Ren, William L. Hamilton, and Jure Leskovec. 2018. Hierarchical Graph Representation Learning with Differentiable Pooling. *arXiv:1806.08804 [cs.LG]*

A RESULTS FOR τ , ρ AND $P@K$

τ and ρ measure how well the predicted results match the ground-truth. For $P@k$, we compute the intersection of predicted top k similar results and the ground-truth top k similar results and divide it by k . As shown in Table 8, it can be found that models under our “CoSim-GNN” framework outperforms matching models and embedding models on almost all the metrics for these five datasets except for $P@20$ on **ER-100**. These results together with the *MSE*, *MAE* and *Time* results show that while our proposed framework significantly reduce the time consumption as compared to matching models, it also outperforms matching models on five evaluation metrics, thus far better than embedding models, demonstrating the efficiency and effectiveness of “CoSim-GNN”.

B GENERATION OF SYNTHETIC DATASETS

We first generate a small number of basic graphs and apply two different categories of pruning rules to prune these graphs for derived graphs. In this section, we will discuss why we follow this process to generate synthetic data and how the two pruning rules work.

B.1 Why we adopt this generation process?

If we generate graphs with a large number of nodes randomly, all these graphs might be highly dissimilar to each other thus the similarity distribution of the graph pairs in the dataset will be uneven (only a very small portion of graph pairs are similar). The generation process we adopt makes the similarity distribution more uniform because derived graphs from the same basic graph can be more similar and meanwhile different basic graphs produce more dissimilar derived graphs.

B.2 BA model and ER model’s Datasets

B.2.1 Barabási-Albert preferential attachment model. Here we introduce the concept of BA-model, the rules for generating a BA-graph, and how our datasets are produced.

BA-model [11] is an algorithm for generating random scale-free networks using a preferential attachment mechanism. Specifically, the BA-model begins with an initial connected network of m_0 nodes. New nodes are added to the network one at a time. Each new node is connected to $m \leq m_0$ existing nodes with a probability that is proportional to the number of links that the existing nodes already have. As a result, the new nodes have a “preference” to attach themselves to the already heavily linked nodes.

Our dataset is made up of some basic graphs and derivative graphs that have been trimmed, which solve several challenges:

- When generating a graph with a large number of nodes randomly, there is a high probability that the generated graphs are dissimilar between each other, which result in an uneven similarity distribution after the normalization described in equation 13.
- Due to the large number of nodes in each graph, the approximate GED algorithm cannot guarantee that the calculated similarity can fully reflect the similarity of the graph pairs. We trim and generate derivative graphs while recording the number of trimming steps. These steps and the values calculated by the approximation algorithm take the minimum

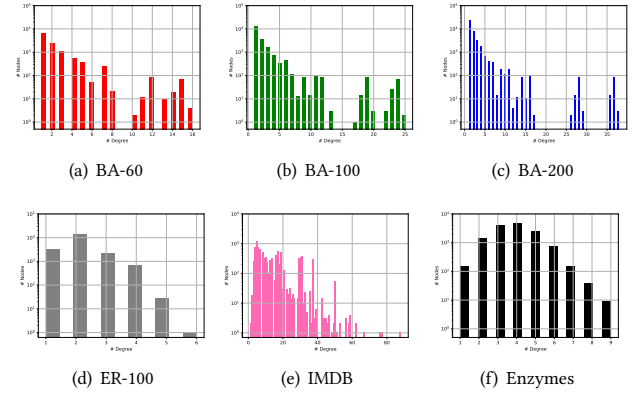


Figure 5: Histogram for statistics of similarity regression datasets.

value as the GED with the basic graph, thereby obtaining a more accurate similarity.

- By trimming different steps, we can generate graphs with different similarities, which is more conducive to the experiment of graph similarity query.

There are three types of trimming methods here: delete a leaf node, add an edge, and add a node. Since deleting an edge may have a greater impact on the result of the generated graph, we will not consider this method. We try to trim the base graph without changing the global features of the base graph to generate more similar graph pairs. In this way, we get three datasets according to the following generation rule.

A BA-graph of n nodes is grown by attaching new nodes each with m edges that are preferentially attached to existing nodes with high degree. We set n to be 60, 100, and 200, respectively, and m is fixed to 1, to generate basic graphs. Each sub-dataset generates two basic graphs, and each base graph is trimmed with different GED distances. For each basic graph, generate 99 trimmed graphs in the range of GED distance 1 to 10. So each sub-dataset consists of two basic graphs and 198 trimmed graphs.

B.2.2 Erdős-Rényi graph or a binomial graph model. In game theory, Erdős-Rényi model stands for either of two similar models for generating random graphs, named respectively after mathematicians Paul Erdős and Alfréd Rényi. The definition of these two models are as follows:

- In the $G(n, M)$ model, a graph is chosen uniformly at random from the collection of all graphs which have n nodes and M edges. For example, in the $G(3, 2)$ model, each of the three possible graphs on three vertices and two edges are included with probability $1/3$.
- In the $G(n, p)$ model, a graph is constructed by connecting nodes randomly. Each edge is included in the graph with probability p independent from every other edge. Equivalently, all graphs with n nodes and M edges have equal probability of $p^M(1-p)^{\frac{n}{2}-M}$. The parameter p in this model can be thought of as a weighting function; as p increases from 0 to 1, the model becomes more and more likely to

Table 8: Results on BA-60, BA-100, BA-200, ER-100 and IMDB datasets

Method	BA-60				BA-100				BA-200				ER-100				IMDB			
	τ	ρ	p@10	p@20																
hungarian	0.5772*	0.7598*	0.7425*	0.8438*	0.6036*	0.8110*	0.6100*	0.9900*	0.5810*	0.7938*	0.6425*	0.9400*	0.3757*	0.5404*	0.6600*	0.7400*	0.8318*	0.9309*	0.7487*	0.8092*
vj	0.0229*	0.0329*	0.3500*	0.5050*	0.4156*	0.5837*	0.4625*	0.8262*	0.4310*	0.6191*	0.4850*	0.8037*	0.2876*	0.4030*	0.5950*	0.6637*	0.8334*	0.9332*	0.7460*	0.8151*
beam	0.7434*	0.8580*	0.6775*	0.9000*	0.6283*	0.7867*	0.6275*	0.9000*	0.6521*	0.7724*	0.5600*	0.8350*	0.4255*	0.5261*	0.5800*	0.6937*	0.9040*	0.9601*	0.9092*	0.9072*
GCN-Mean	0.5329	0.7564	0.5800	0.8688	0.5338	0.7639	0.5650	1.0000	0.4946	0.7347	0.5000	0.9500	0.4708	0.6704	0.5175	0.7862	0.3620	0.4664	0.4868	0.7026
GCN-Max	0.5230	0.7461	0.5450	0.8662	0.5304	0.7617	0.5250	0.9987	0.5169	0.7499	0.5375	0.9425	0.4313	0.6244	0.5150	0.7738	0.1736	0.2462	0.3908	0.4460
SimGNN	0.5678	0.7730	0.7100	0.8887	0.5383	0.7637	0.5800	1.0000	0.4889	0.7347	0.5275	0.9513	0.5848	0.7212	0.6575	0.8177	0.3935	0.5270	0.5566	0.6158
GSimCNN	0.6048	0.8078	0.6775	0.9050	0.5932	0.8079	0.6450	1.0000	0.5761	0.7958	0.6075	0.9500	0.6093	0.8041	0.7100	0.8488	0.4987	0.6626	0.6210	0.6414
GMN	0.5601	0.7753	0.6150	0.8800	0.5499	0.7755	0.5675	1.0000	0.6034	0.8140	0.6375	0.9500	0.6538	0.8363	0.7650	0.8875	0.5538	0.6956	0.6566	0.7187
CoSim-CNN	0.6059	0.8057	0.7475	0.9050	0.6335	0.8332	0.7100	1.0000	0.6020	0.8092	0.6850	0.9512	0.5998	0.8012	0.7050	0.8150	0.5499	0.6855	0.6421	0.7032
CoSim-ATT	0.6076	0.8083	0.6580	0.8887	0.6063	0.8146	0.6550	1.0000	0.6315	0.8330	0.6950	0.9525	0.6226	0.8178	0.7800	0.8025	0.6051	0.7237	0.6632	0.7343
CoSim-SAG	0.6282	0.8221	0.6925	0.8937	0.6265	0.8313	0.6650	1.0000	0.5593	0.7837	0.5575	0.9500	0.5451	0.7251	0.6333	0.8265	0.6287	0.7628	0.6934	0.7671
CoSim-TOPK	0.6081	0.8059	0.6250	0.9175	0.5962	0.8073	0.5850	1.0000	0.5589	0.7822	0.5889	0.9500	0.5726	0.7775	0.7075	0.8175	0.5802	0.7155	0.6118	0.6941
CoSim-MEM	0.5529	0.7704	0.5625	0.8837	0.5763	0.7962	0.6275	1.0000	0.6184	0.8252	0.7025	0.9512	0.6481	0.8308	0.7975	0.8100	0.6057	0.7486	0.6434	0.7520
CoSim-GNN10	0.6485	0.8332	0.8000	0.8775	0.6261	0.8315	0.6475	1.0000	0.5950	0.8097	0.6875	0.9500	0.6649	0.8520	0.7775	0.8500	0.6629	0.8050	0.6868	0.7697
CoSim-GNN1	0.6375	0.8297	0.7750	0.9000	0.6076	0.8144	0.6525	1.0000	0.6060	0.8150	0.6275	0.9550	0.6478	0.8304	0.7806	0.8363	0.6989	0.8277	0.7276	0.7816

include graphs with more edges and less and less likely to include graphs with fewer edges. In particular, the case $p = 0.5$ corresponds to the case where all $2^{\frac{n}{2}}$ graphs on n vertices are chosen with equal probability.

A ER-graph connects each pair of n nodes with probability p . Like the BA model, we set n to be 100, and adjust the value of p so that the graph is not too dense. We generate the base graphs and trim them in the same way, so each dataset consists of two basic graphs and 198 pruned graphs too.

C STATISTICS OF DATASETS

Statistics of graph-graph similarity regression datasets used in this paper are presented in Fig. 5 and Table 9.

Dataset	Min Nodes	Max Nodes	Avg Nodes	Min Edges	Max Edges	Avg Edges
BA-60	54	65	59.50	54	66	60.06
BA-100	96	105	100.01	96	107	100.56
BA-200	192	205	199.63	193	206	200.16
ER-100	94	104	99.90	98	107	101.43
IMDB	15	89	24.10	33	1467	166.58
Enzymes	30	125	42.84	42	149	81.47

D DEVICE INFORMATION USED IN THE EXPERIMENTS

We use a desktop computer with 6 Intel(R) i5-8600K@3.60GHz CPU cores. We here do not use GPU for acceleration because our experiments show that GPU do not significantly make the learning process faster under our data framework. Note that all experiments in Fig. 4 are conducted on a different computer.

E NEW BENCHMARKS FOR GRAPH-GRAF SIMILARITY COMPUTATION

In this work, we create a set of synthetic datasets and real-world datasets to study large-scale graph similarity computation. These datasets provide new benchmarks since lacking accurate labels for graph-graph similarity is one of the biggest problem that hinders the development of the field of large-scale graph similarity computation. Detail reasons are as follows.

The first one is the time and memory consumption. It is hard to get graph similarity computation benchmarks mainly because it is quite hard to get the ground truth (labels). To calculate the approximate GED ground truth values of graph pairs, we use the same mechanism as that in [1]. This mechanism runs in sub-exponential time complexity and has a high memory cost, it is inapplicable to get the ground truths if each graph contains more than hundreds of nodes. Thus graphs in our selected datasets have 20 to 200 nodes and it takes several days to compute the ground truths for each dataset. What's more, if graphs are too dense, it will also lead to high computational burden when generating labels.

The second one lies in the unbalanced distribution in real-world graph datasets. In many datasets, most of the graph pairs are dissimilar, which result in an uneven similarity distribution after normalization where most of the ground-truth similarities are close to 0. Thus the deep neural network might tend to always output 0 to minimize the loss without actually extracting meaningful representation for graphs.

The third problem is that the approximate GED algorithms are not always accurate especially when the two graphs are large. With synthetic datasets, we can trim and generate derivative graphs while recording the number of trimming steps. We then take the minimum value among this number and the values calculated by the approximation algorithms as the GED with the basic graph, thereby obtaining a more accurate ground-truth similarity.